ORIGINAL RESEARCH ■ NEURORADIOLOGY

Radiology

Idiopathic Normal-Pressure Hydrocephalus: Temporal Changes in ADC during Cardiac Cycle[1]

Naoki Ohno, MS
Tosiaki Miyati, PhD, DMSc
Mitsuhito Mase, MD, PhD
Tomoshi Osawa, MD, PhD
Hirohito Kan, MS
Harumasa Kasai, MS
Masaki Hara, MD, PhD
Yuta Shibamoto, MD, PhD
Norio Hayashi, PhD
Toshifumi Gabata, MD, PhD
Osamu Matsui, MD, PhD

Purpose: To determine whether temporal changes in apparent diffusion coefficient (ADC) over the cardiac cycle are different in patients with idiopathic normal-pressure hydrocephalus (INPH) as compared with patients with ex vacuo ventricular dilatation and healthy control subjects.

Materials and Methods: This prospective study was approved by the institutional review board and was performed only after informed consent was obtained from each patient. At 1.5 T, electrocardiographically triggered single-shot diffusion echo-planar magnetic resonance imaging (b = 0 and 1000 sec/mm^2) was performed with sensitivity encoding and half-scan techniques to minimize bulk motion. ΔADC was defined as the difference between maximum and minimum ADC on a pixel-by-pixel basis over 20 phases of the cardiac cycle. Mean ADC during the diastolic phase and ΔADC in the frontal white matter were determined in patients with INPH (n = 13), patients with ex vacuo ventricular dilatation (n = 8), and healthy volunteers (n = 10). Kruskal-Wallis tests were used to determine significance between groups.

Results: Mean ΔADC in the INPH group was significantly higher than that in the ex vacuo ventricular dilatation and control groups ($P < .01$ for both). There was no significant difference in ΔADC between the ex vacuo ventricular dilatation and control groups ($P = .86$). There was no significant difference in mean ADC during the diastolic phase among groups ($P > .05$ for all). There was no significant correlation between ΔADC and mean ADC during the diastolic phase in any group.

Conclusion: Determination of fluctuation of ADC over the cardiac cycle may render it possible to noninvasively obtain new and more detailed information than that provided by standard ADC measurement in suspected INPH, potentially facilitating the diagnosis of this disease.

© RSNA, 2011

Normal-pressure hydrocephalus (NPH) is characterized by a clinical triad of ataxia, incontinence, and dementia, as well as dilated ventricles but normal cerebrospinal fluid (CSF) pressures. In patients with NPH, CSF shunt placement is effective for improving these symptoms (1). NPH has attracted attention as one of the few treatable causes of dementia. Diagnosis of idiopathic NPH (INPH) without a known cause of communicating hydrocephalus, including subarachnoid hemorrhage or meningitis, is particularly difficult (2). Moreover, to clarify the cause of NPH, accurately diagnose NPH, and identify appropriate patients for shunt surgery, several tests have been proposed, including cisternography, the CSF tap test, resistance measures, external lumbar drainage, and intracranial pressure recording, in addition to clinical findings and conventional imaging diagnosis with x-ray computed tomography or magnetic resonance (MR) imaging (3–6). It has also been reported (7) that a single standard for the prognostic evaluation of patients with INPH was lacking and that supplemental tests could increase the predictive accuracy of the prognosis. The CSF tap test is a particularly reliable examination, but it is invasive and has low sensitivity. It has been proposed that MR imaging CSF flow studies can be used to noninvasively obtain information about intracranial mechanical properties in INPH (eg, intracranial compliance) (2,8–12). However, the diagnostic utility of this latter method is still not established.

Arterial inflow into the cranium induces venous and CSF outflow and displacement of the intracranial spinal cord during the cardiac cycle, resulting in pulsatile brain motion (12–14). Brain pulsation (ie, bulk motion) reportedly can give rise to artifactual phase dispersion and may lead to overestimation of the apparent diffusion coefficient (ADC) (15,16). Brockstedt et al (17) reported that ADC was not changed significantly during the cardiac cycle with the single-shot echo-planar imaging (EPI) sequence widely used in diffusion MR imaging. However, they analyzed only two delay times (100 and 400 msec) between the R peaks in the cardiac cycle. To more completely analyze ADC changes during the cardiac cycle, our own group has previously evaluated the temporal change in ADC during the entire cardiac cycle by using an electrocardiographically (ECG)-triggered single-shot diffusion EPI sequence to minimize bulk motion effect. As a result, we revealed in a previous study that white matter ADC changed significantly over the cardiac cycle and that such changes were synchronized with the arterial inflow (volume loading) at systole (18). We further hypothesize that changes in ADC during the cardiac cycle are related to the biomechanical properties of intracranial tissues; hence, observed temporal changes in ADC in diseases such as INPH that are characterized by low intracranial compliance (12) may well be different than those in other diseases. Therefore, the purpose of our study was to determine whether temporal changes in ADC over the cardiac cycle were different in patients with INPH as compared with patients with ex vacuo ventricular dilatation and healthy control subjects.

Materials and Methods

Subjects

The purpose and procedures of all our investigations were fully explained to all patients, and the studies were performed only after we obtained informed consent from each patient. This study was approved by the institutional review board at Nagoya City University. In this prospective study, 13 patients with INPH (nine men and four women; mean age, 78 years; range, 71–84 years), eight patients with ex vacuo ventricular dilatation with an Evans index greater than 0.3 (five men and three women; mean age, 76 years; range, 68–80 years), and 10 healthy volunteers (four men and six women; mean age, 72 years; range, 67–80 years) were examined between June 2009 and February 2011 (Table). No patient was excluded from the study. The diagnosis of INPH was confirmed by two neurosurgeons (M.M. and T.O., with 25 and 10 years of experience in neurosurgery, respectively) and was

Advances in Knowledge

- Temporal changes in the brain parenchyma's apparent diffusion coefficient (ADC) during the cardiac cycle (ΔADC) reveal the degree of fluctuation of water molecules likely resulting from arterial inflow (volume loading) during systole.

- The increased fluctuation of water molecules in the brain parenchyma due to diminished compliance may explain elevated mean ΔADC in the idiopathic normal-pressure hydrocephalus (INPH) group as compared with that in the patients with ex vacuo ventricular dilatation and the control group.

Implication for Patient Care

- Analysis of temporal changes in ADC over the cardiac cycle may render it possible to noninvasively obtain new and more detailed information than that provided by standard ADC measurement in suspected INPH, potentially facilitating the diagnosis of this disease.

based on evidence from the clinical examination, brain imaging, and CSF tap test according to the Japanese guidelines set by Ishikawa et al (19). All patients with INPH showed improvement after a CSF tap test, according to symptom analysis after lumbar puncture and removal of CSF. Nine of 13 patients with INPH showed clinical improvement after shunt surgery. For four of 13 patients, shunt surgery was not performed because we could not obtain informed consent.

Procedure for ∆ADC Analysis

ECG-triggered single-shot diffusion MR imaging was performed to calculate the ADC map in each cardiac phase by two authors (H. Kasai and H. Kan, with 15 and 2 years of experience in MR imaging, respectively). The trigger delay was set at regular intervals depending on the heart rate (approximately 20 cardiac phases). Multiphase diffusion-weighted images were acquired over multiple heartbeats. The ADC was calculated by using the following equation: $ADC = \ln(S_1/S_2)/b_2 - b_1$, where b_1 and b_2 represent the parameters of the diffusion gradient and S_1 and S_2 represent signal intensities at each respective b value. Maximum change in ADC (∆ADC) was calculated from all cardiac phase images (20 phases) on a pixel-by-pixel basis by using the following equation: $\Delta ADC = ADC_{max} - ADC_{min}$, where ADC_{max} and ADC_{min} represent the maximum and minimum ADC during the cardiac cycle. A ∆ADC image was created. We then determined mean ∆ADC in regions of interest (ROIs) on the ∆ADC image. The ROI was drawn manually in the frontal white matter defined on a high-spatial-resolution T2-weighted image at the same section level as the ∆ADC image to exclude the periventricular high-signal-intensity area on the T2-weighted image by one of three authors (M.M., N.O., and T.M., with 25, 4 and 25 years of experience in MR imaging, respectively) with mutual consent of the other two authors. The mean ROI size was 85 mm² (range, 60–120 mm²). Because white matter regions other than those in the frontal white matter were extremely small in patients with INPH and patients with ex vacuo ventricular dilatation,

we did not evaluate them to avoid the partial volume effect. We compared mean ∆ADC in the frontal white matter among the INPH, ex vacuo ventricular dilatation, and control groups. In addition to the ∆ADC analysis, we also compared mean ADC of the diastolic phases between groups (20).

Image Acquisition

With a 1.5-T MR imaging unit (Gyroscan Intera; Philips Medical Systems, Best, the Netherlands), ECG-triggered single-shot diffusion EPI was performed with the following parameters: repetition time, two R-R intervals; echo time 70 msec; flip angle, 90°; section thickness, 4 mm; imaging matrix, 64 × 64; field of view, 256 mm; number of signals averaged, two; 20 cardiac phases (different phases acquired by varying ECG trigger delay time); $b = 0$ and 1000 sec/mm²; duration and respective times between leading edges of the diffusion gradients, 28.6 and 48.7 msec; three separate measures in the x-, y-, and z-axis directions; sensitivity encoding factor, two; and half-scan factor, 0.6. In single-shot EPI, all k-space data are acquired with only a single radiofrequency excitation.

Demographic Data, Mean ∆ADC, and ADC in Frontal White Matter in All Subjects

Group and Patient No./ Sex/Age (y)	∆ADC (× 10⁻³ mm²/sec)	ADC (× 10⁻³ mm²/sec)
Control		
1/F/57	0.186	0.762
2/F/67	0.238	0.773
3/F/77	0.172	0.797
4/F/71	0.200	0.713
5/M/67	0.259	0.741
6/M/80	0.267	0.732
7/M/75	0.275	0.759
8/F/70	0.232	0.726
9/F/77	0.220	0.793
10/M/77	0.385	0.778
INPH*		
11/M/81	0.340	0.801
12/F/75	0.275	0.773
13/M/77	0.425	0.813
14/M/70	0.394	0.804
15/M/76	0.328	0.737
16/M/84	0.333	0.747
17/F/81	0.331	0.781
18/M/71	0.240	0.771
19/M/77	0.328	0.757
20/F/74	0.434	0.737
21/M/84	0.448	0.726
22/F/81	0.407	0.785
23/M/78	0.241	0.744
Ex vacuo ventricular dilatation		
24/M/78	0.254	0.803
25/M/81	0.144	0.793
26/F/68	0.204	0.687
27/M/79	0.230	0.737
28/F/74	0.255	0.780
29/M/80	0.276	0.853
30/F/70	0.196	0.642
31/F/77	0.273	0.773

*Patients 12, 14, 15, 18, 19, 20, 21, 22, and 23 had a positive shunt response, while patients 11, 13, 16, and 17 did not undergo surgery.

Generally, single-shot EPI allows acquisition of an image within 80 msec and hence is largely insensitive to motion (21). However, it is difficult to eliminate the bulk motion effect completely with single-shot EPI alone because the data sampling window is extended by increasing echo train length. Moreover, this technique is susceptible to image blurring and distortion. To resolve these problems, we used half-scan, rectangular field of view, and sensitivity encoding techniques (22). Thus the duration of the data sampling window could be 8.5 msec.

Statistical Analyses

All statistical analyses were performed by using software (SPSS for Windows, version 18.0; SPSS, Chicago, Ill). Kruskal-Wallis tests were used to determine the significance between groups. The relation between the ΔADC and ADC was assessed by using multiple linear regression analysis. $P < .05$ was considered to indicate a significant difference.

Results

Demographic data are shown in the Table. Examples of mean ADC in the frontal white matter during the cardiac cycle and ΔADC images in each group are shown in Figure 1. The ADCs in the frontal white matter changed significantly during the cardiac cycle in each group ($P < .01$ for all).

Figure 2 shows the mean ΔADCs of the frontal white matter in patients with INPH, patients with ex vacuo ventricular dilatation, and the control group. The mean ΔADC of the INPH group was 0.348×10^{-3} mm²/sec ± 0.070 (standard deviation), compared with 0.229×10^{-3} mm²/sec ± 0.045 for the ex vacuo ventricular dilatation group and 0.243×10^{-3} mm²/sec ± 0.060 for the control group. Mean ΔADC in the INPH group was significantly greater than that in the ex vacuo ventricular dilatation and control groups ($P < .01$ for both), whereas there was no signif-

icant difference in ΔADC between the ex vacuo ventricular dilatation and control groups ($P = .86$).

Figure 3 shows the mean ADCs during the diastolic phase in the frontal white matter in patients with INPH, patients with ex vacuo ventricular dilatation, and the control group. The mean ADC of the INPH group was 0.767×10^{-3} mm²/sec ± 0.028, compared with 0.758×10^{-3} mm²/sec ± 0.068 for the ex vacuo ventricular dilatation group and 0.757×10^{-3} mm²/sec ± 0.029 for the control group. There was no significant difference in ADC between the INPH and ex vacuo ventricular dilatation groups ($P = .93$), the INPH and control groups ($P = .44$), and the ex vacuo ventricular dilatation and control groups ($P = .55$).

The relationship between ΔADC and ADC in white matter is shown in Figure 4. There was no significant correlation between ΔADC and ADC (INPH group, $P = .81$; ex vacuo ventricular dilatation group, $P = .28$; control group, $P = .95$).
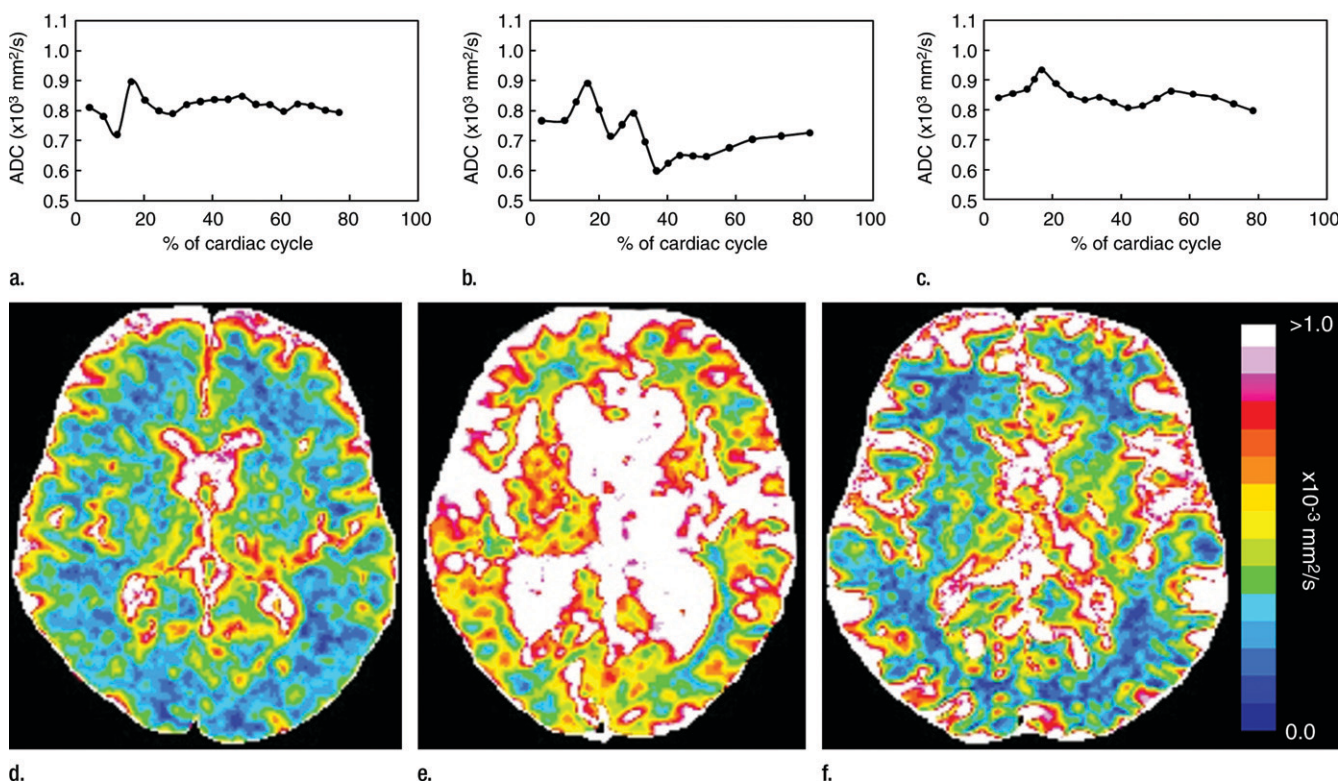
Figure 1

Figure 1: (a–c) Graphs of ADC changes during the cardiac cycle and (d–f) ΔADC images show typical study findings in (a, d) a healthy 67-year-old man, (b, e) a 76-year-old man with INPH, and (c, f) a 78-year-old man with ex vacuo ventricular dilatation.

Discussion

In the current study, we demonstrated that mean ADCs changed significantly over the cardiac cycle in multiple patient groups, apparently altered by the arterial inflow (volume loading) at systole, even with minimization of the effect of bulk motion (18). We further demonstrated that changes in ADC over the cardiac cycle were more pronounced in patients with INPH than in either healthy control subjects or patients with ex vacuo ventricular dilatation. This latter observation suggests that the diminished intracranial compliance in INPH as compared with that in the other groups led to tight mechanical coupling between blood flow and CSF pulsation in the cardiac cycle (23); hence, water molecules in the brain parenchyma were substantially impacted by the volume loading. We propose that temporal changes in

ADC over the cardiac cycle may not only provide a reliable diagnostic test for INPH but also allow selection of appropriate patients for shunt surgery in this condition.

The observed differences in ΔADC among groups may be explained as follows: Brain expansion is induced by dilation of the intracranial arterial vessels, which causes intracranial volume loading. Greitz et al (24) investigated brain motion by using phase-contrast MR imaging and verified that volume loading induces brain displacement toward the ventricular system. In healthy brains, this volume loading is dampened by venous and CSF outflow, as well as by displacement of the intracranial spinal cord from the cranium. Furthermore, many studies (2,8–12) have demonstrated reduced compliance in INPH. Bateman et al (25) reported that venous resistance is increased; that is, venous compliance is decreased as a consequence of the low intracranial compliance. The dampening of the brain pulsation by the venous

system is decreased because of reduced venous compliance; alternatively, the increased CSF outflow allows dampening of the excess volume loading (26). The pulsation force not dampened by the venous outflow is propagated directly into the brain parenchyma, and, as a result, increased brain expansion is directed inward and compresses the ventricles. The increased "fluctuation" of water molecules in the brain parenchyma because of low compliance may explain the elevated mean ΔADC in the INPH group as compared with that in the ex vacuo ventricular dilatation and control groups. Moreover, INPH reportedly increases the amount of water in the extracellular space used as an alternative CSF absorption pathway (27). We consider that this increased amount of water in the extracellular space in INPH may also render the water molecular fluctuation greater and mean ΔADC higher.

In the present study, we detected no significant difference in mean ADC among groups. Thus, the fact that mean ΔADC in the INPH group was significantly higher than that in the control and ex vacuo ventricular dilatation groups despite the former finding indicates the utility of the ΔADC analysis. Furthermore, the lack of significant correlation between mean ΔADC and ADC suggests that ΔADC and ADC do not necessarily provide the same kind of information— that is, the ΔADC reveals the degree of fluctuation of water molecules resulting from volume loading at systole. Although dynamic change in the ADC during the cardiac cycle has been thought to result in artifacts, we considered that the ΔADC analysis provided new information
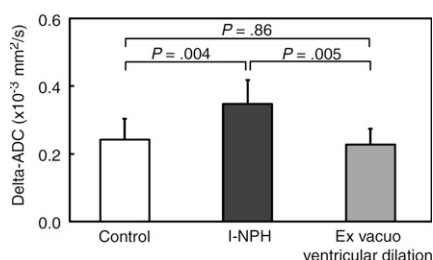
Figure 2

Figure 2: Bar graph shows mean ΔADCs in each group. Mean ΔADC in the INPH group was significantly higher than that in the ex vacuo ventricular dilatation and control groups ($P < .01$ for both), whereas there was no significant difference in ΔADC between the ex vacuo ventricular dilatation and control groups ($P = .86$). Error bars = standard deviations.
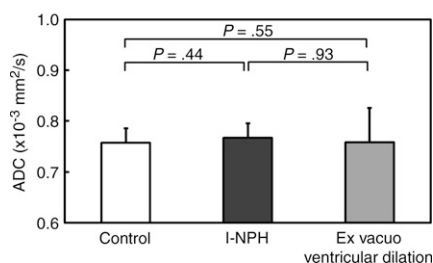
Figure 3

Figure 3: Bar graph shows mean ADCs in each group. There was no significant difference in ADC between groups ($P > .05$ for all). Error bars = standard deviations.
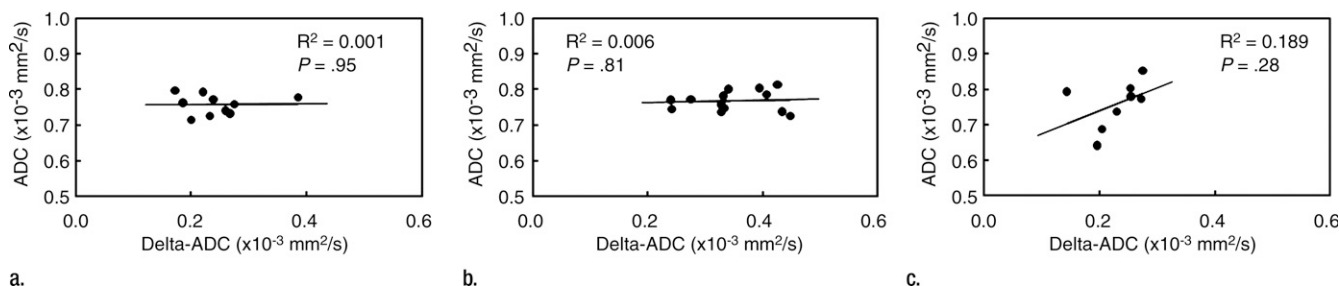
Figure 4

a.

b.

c.

Figure 4: Relationship between ΔADC and ADC in **(a)** healthy volunteers, **(b)** patients with INPH, and **(c)** patients with ex vacuo ventricular dilatation. There was no significant correlation between ΔADC and ADC ($P > .05$ for all).

as compared with standard diffusion parameters and thus may facilitate assessment of diseases as a new biomarker in which ADC remains normal. The ΔADC data can be obtained within 10 minutes, and each ADC image is also used for diagnosis, thereby making for easier clinical application.

Our study had several limitations. First, because the patient populations were small, we recommend that further evaluation be undertaken with a larger sample size to confirm the efficacy of the method described in this study. Second, the alteration in ΔADC and ADC induced by age differences was not clarified in this study. Further investigation with a wider age range should be pursued in future. Third, we plan to improve the pulse sequence with a shorter acquisition time, an optimized combination of b values for obtaining accurate ADCs, and lower noise than in the current series.

In conclusion, we evaluated the change in ADC during the cardiac cycle in patients with INPH in comparison with the ADC in healthy subjects and patients with ex vacuo ventricular dilatation. The mean ΔADC in the INPH group was significantly higher than that in the control and ex vacuo ventricular dilatation groups, whereas there was no significant difference in ADC between groups. Determination of fluctuation of ADC over the cardiac cycle may render it possible to noninvasively obtain new and more detailed information than that provided by the standard ADC measurement in suspected INPH, potentially facilitating the diagnosis of this disease.

References

1. Adams RD, Fisher CM, Hakim S, Ojemann RG, Sweet WH. Symptomatic occult hydrocephalus with "normal" cerebrospinal-fluid pressure: a treatable syndrome. N Engl J Med 1965;273:117–126.

2. Bateman GA, Levi CR, Schofield P, Wang Y, Lovett EC. The pathophysiology of the aqueduct stroke volume in normal pressure hydrocephalus: can co-morbidity with other forms of dementia be excluded? Neuroradiology 2005;47(10):741–748.

3. Raftopoulos C, Chaskis C, Delecluse F, Cantraine F, Bidaut L, Brotchi J. Morphological quantitative analysis of intracranial pressure waves in normal pressure hydrocephalus. Neurol Res 1992;14(5):389–396.

4. Vanneste J, Augustijn P, Davies GA, Dirven C, Tan WF. Normal-pressure hydrocephalus: is cisternography still useful in selecting patients for a shunt? Arch Neurol 1992;49(4):366–370.

5. Boon AJ, Tans JT, Delwel EJ, et al. Dutch normal-pressure hydrocephalus study: prediction of outcome after shunting by resistance to outflow of cerebrospinal fluid. J Neurosurg 1997;87(5):687–693.

6. Walchenbach R, Geiger E, Thomeer RT, Vanneste JA. The value of temporary external lumbar CSF drainage in predicting the outcome of shunting on normal pressure hydrocephalus. J Neurol Neurosurg Psychiatry 2002;72(4):503–506.

7. Marmarou A, Bergsneider M, Klinge P, Relkin N, Black PM. The value of supplemental prognostic tests for the preoperative assessment of idiopathic normal-pressure hydrocephalus. Neurosurgery 2005;57(3 Suppl):S17–S28; discussion ii–v.

8. Matsumoto T, Nagai H, Kasuga Y, Kamiya K. Changes in intracranial pressure (ICP) pulse wave following hydrocephalus. Acta Neurochir (Wien) 1986;82(1-2):50–56.

9. Miyati T, Mase M, Banno T, et al. Frequency analyses of CSF flow on cine MRI in normal pressure hydrocephalus. Eur Radiol 2003;13(5):1019–1024.

10. Balédent O, Gondry-Jouet C, Meyer ME, et al. Relationship between cerebrospinal fluid and blood dynamics in healthy volunteers and patients with communicating hydrocephalus. Invest Radiol 2004;39(1):45–55.

11. Greitz D. Radiological assessment of hydrocephalus: new theories and implications for therapy. Neurosurg Rev 2004;27(3):145–165; discussion 166–167.

12. Miyati T, Mase M, Kasai H, et al. Noninvasive MRI assessment of intracranial compliance in idiopathic normal pressure hydrocephalus. J Magn Reson Imaging 2007;26(2):274–278.

13. Alperin N, Vikingstad EM, Gomez-Anson B, Levin DN. Hemodynamically independent analysis of cerebrospinal fluid and brain motion observed with dynamic phase contrast MRI. Magn Reson Med 1996;35(5):741–754.

14. Alperin NJ, Lee SH, Loth F, Raksin PB, Lichtor T. MR-intracranial pressure (ICP): a method to measure intracranial elastance and pressure noninvasively by means of MR imaging: baboon and human study. Radiology 2000;217(3):877–885.

15. Anderson AW, Gore JC. Analysis and correction of motion artifacts in diffusion weighted imaging. Magn Reson Med 1994;32(3):379–387.

16. Wirestam R, Greitz D, Thomsen C, Brockstedt S, Olsson MB, Stahlberg F. Theoretical and experimental evaluation of phase-dispersion effects caused by brain motion in diffusion and perfusion MR imaging. J Magn Reson Imaging 1996;6(2):348–355.

17. Brockstedt S, Borg M, Geijer B, et al. Triggering in quantitative diffusion imaging with single-shot EPI. Acta Radiol 1999;40(3):263–269.

18. Nakamura T, Miyati T, Kasai H, et al. Bulk motion-independent analyses of water diffusion changes in the brain during the cardiac cycle. Radiol Phys Technol 2009;2(2):133–137.

19. Ishikawa M, Hashimoto M, Kuwana N, et al. Guidelines for management of idiopathic normal pressure hydrocephalus. Neurol Med Chir (Tokyo) 2008;48(Suppl):S1–S23.

20. Skare S, Andersson JL. On the effects of gating in diffusion imaging of the brain using single shot EPI. Magn Reson Imaging 2001;19(8):1125–1128.

21. Norris DG. Implications of bulk motion for diffusion-weighted imaging experiments: effects, mechanisms, and solutions. J Magn Reson Imaging 2001;13(4):486–495.

22. Bammer R, Keeling SL, Augustin M, et al. Improved diffusion-weighted single-shot echo-planar imaging (EPI) in stroke using sensitivity encoding (SENSE). Magn Reson Med 2001;46(3):548–554.

23. Stoquart-ElSankari S, Balédent O, Gondry-Jouet C, Makki M, Godefroy O, Meyer ME. Aging effects on cerebral blood and cerebrospinal fluid flows. J Cereb Blood Flow Metab 2007;27(9):1563–1572.

24. Greitz D, Wirestam R, Franck A, Nordell B, Thomsen C, Ståhlberg F. Pulsatile brain movement and associated hydrodynamics studied by magnetic resonance phase imaging: the Monro-Kellie doctrine revisited. Neuroradiology 1992;34(5):370–380.

25. Bateman GA, Levi CR, Schofield P, Wang Y, Lovett EC. The venous manifestations of pulse wave encephalopathy: windkessel dysfunction in normal aging and senile dementia. Neuroradiology 2008;50(6):491–497.

26. Bateman GA. The pathophysiology of idiopathic normal pressure hydrocephalus: cerebral ischemia or altered venous hemodynamics? AJNR Am J Neuroradiol 2008;29(1):198–203.

27. Bradley WG Jr, Bahl G, Alksne JF. Idiopathic normal pressure hydrocephalus may be a "two hit" disease: benign external hydrocephalus in infancy followed by deep white matter ischemia in late adulthood. J Magn Reson Imaging 2006;24(4):747–755.